

1 Article

2 Condition Monitoring of Bearing Faults Using the 3 Stator Current and Shrinkage Methods

4 Oscar Duque-Perez^{1,*}, Carlos Del Pozo-Gallego¹, Daniel Morinigo-Sotelo¹, Wagner Fontes
5 Godoy²

6 ¹ Department of Electrical Engineering. University of Valladolid. Valladolid, Spain;

7 ² Department of Electrical Engineering. Universidade Tecnológica Federal do Parana. Cornelio Procopio,
8 Brazil;

9 * Correspondence: oscar.duque@eii.uva.es

10

11 **Abstract:** Condition monitoring of bearings is an open issue. The use of the stator current to monitor
12 induction motors has been validated as a very advantageous and practical way to detect several
13 types of faults. Nevertheless, for bearing faults the use of vibrations or sound generally offers better
14 results in the accuracy of the detection although with some disadvantages related to the sensors
15 used for monitoring. To improve the performance of bearing monitoring, it is proposed to take
16 advantage of more information available in the current spectra, beyond the usually employed,
17 incorporating the amplitude of a significant number of sidebands around the first eleven harmonics,
18 growing exponentially the number of fault signatures. This is especially interesting for inverter-fed
19 motors. But, in turn, this leads to the problem of overfitting when applying a classifier to perform
20 the fault diagnosis. To overcome this problem, and still exploit all the useful information available
21 in the spectra, it is proposed to use shrinkage methods, which have been lately proposed in machine
22 learning to solve the overfitting issue when the problem has much more variables than examples to
23 classify. A case study with a motor is shown to prove the validity of the proposal.

24 **Keywords:** condition monitoring, bearings, machine learning, current spectra.

25

26 1. Introduction

27 Induction motors are a fundamental part of many production processes due to their inherent
28 robustness, low cost and reliability, among other advantages. However, they are not fault-free, with
29 bearings being the component that accounts for the greatest percentage of total failures [1].

30 The signals that are most frequently used for bearing fault detection are vibration and acoustic
31 noise [2]. However, the use of the stator current to monitor the motor provides some practical
32 advantages related to the simplicity and non-invasive characteristics of the sensors. These advantages
33 are especially relevant in industrial facilities where some motors can run simultaneously [3,4]. The
34 use of current has proven its effectiveness in detecting faults such as broken bars and eccentricity [2],
35 but in the case of faulty bearings, it faces technical difficulties that hinder its successful
36 implementation. Mainly, the low energy of the vibrations associated to the fault, which makes it
37 difficult to distinguish in the current spectrum the frequency components related to the fault that
38 may be buried in the noise [1,5,6]. Besides, for inverter-fed motors the noise is higher and there are
39 other harmonics present in the spectrum which complicates even more the detection of the faulty
40 related components [7]. Consistently, in [8] denoising techniques are applied to highlight the faulty
41 components in the current spectrum. Other advanced spectral techniques have also been proposed
42 such as wavelets [9,10], Short-Time Fourier Transform [11], Gabor spectrogram [11] Hilbert-Huang
43 Transform [12], Empirical Mode Decomposition [13] MUSIC [13,14], space vector angular fluctuation
44 method [15]. These techniques have the drawback of a high computational cost.

45 The first stage related to the detection of the fault provides with some fault signatures that will
46 feed the second stage of the process, the diagnosis. A wide variety of algorithms has been proposed
47 to diagnose faulty bearings such as Artificial Neural Networks [16,17], Support Vector Machines [12],
48 [18,19], K-nearest neighbors [20,21], supervised fuzzy-neighborhood density-based clustering [22],
49 random forest [23], bagging, boosting and stacking methods [24], Common Vector Approach [25],
50 Decision Trees [26,27]. Maximum margin classification [28], Bayes classifier [29], Euclidean Distance
51 Minimization [30] and Bayesian inference [31]. The aforementioned algorithms were mostly applied
52 making use of the known fault signatures related to bearing faults, limited to just a few signatures
53 (usually just the sideband around the main harmonic, as it will be shown in Section 2). However, for
54 challenging cases this is a restricted use of the information available in the spectra. In the case of
55 inverter-fed motors, it can be used the information related to sidebands around the harmonics
56 introduced by the supply [3]. In [32] it is shown how the effects of different types of bearing faults
57 are spread over the spectrum, being for some cases more notorious for the 3rd and 7th harmonics and,
58 in other cases, for high frequency odd harmonics; besides, these effects are different depending on
59 the operating characteristics of the motor. In [33] the cases of excessive and defective lubrication are
60 analyzed showing how these situations produce changes in the amplitudes of different sidebands
61 around different harmonics, showing also a variation depending on the load.

62 Consequently, in this paper it is proposed to take advantage of the information available over
63 the spectrum, considering not only the main frequency but also different odd and even harmonics
64 (up to the 11th one) and including many more sidebands than is usual in literature. This way, instead
65 of using just a few signatures to feed the algorithm as is usual in literature, almost one thousand
66 signatures are used in this proposal.

67 The drawback of feeding the classifier with a high number of signatures is a clear risk of
68 overfitting. Overfittings arises when the model has learned the data too well, leading to a small error
69 in the training set (used to build the model) but poor prediction ability. Besides, overfitting is
70 intensified by the presence of noise in the data [34] and, precisely, dealing with motors fed from
71 inverters, a significant presence of noise is to be expected. A solution to minimize the overfitting
72 problem is to apply shrinkage techniques. These techniques perform shrinking the values of the
73 coefficients in the trained model. There are several versions of shrinkage techniques depending on
74 the degree of shrinkage of each coefficient. If some of them can be set to zero, then the method is
75 known as Lasso (Least Absolute Shrinkage and Selection Operator) and consequently the number of
76 signatures in the classifier is reduced, obtaining simpler models. If the value of the coefficients is
77 reduced, but all the signatures are included in the model, the method is known as Ridge Regression.
78 The technique known as Elastic Nets is a way of combining both Lasso and Ridge Regression.

79 To monitor correctly the state of the bearings and be really useful for maintenance purposes it is
80 essential to be able to distinguish between different states of deterioration and detect incipient
81 faults before they develop into critical ones. With this purpose, it has been simulated in the laboratory
82 a progressive deterioration of an induction motor bearing via the contamination of the lubrication
83 introducing particles of silicon carbide in the bearing grease. This process tries to emulate conditions
84 usually present in the industry that produces bearing wear related to the use, to inadequate
85 lubrication or to the proper contamination of the grease in open ball bearings.

86 In this paper, it is proposed the use of a large number of fault signatures obtained from the
87 current spectra to monitor bearing failures. A case study is presented where five states of
88 deterioration of the bearing are considered giving rise to a problem of multiclassification. The
89 improved in the performance of different classifiers when using such fault signatures is shown by
90 comparing with the performance with the usual signatures used in these studies. Then, to deal with
91 the problem of overfitting, shrinkage techniques are applied, comparing the performance of Lasso,
92 Ridge Regression and Elastic Nets, proving their validity to diagnose bearing failures.

93 2. Fault Signatures

94 When a bearing defect appears, a radial motion between rotor and stator will occur modifying
95 the airgap of the motor thus changing the airgap field. These modifications in the airgap can be

96 interpreted as a combination of bidirectional rotating eccentricities [35], which implies that the defect
 97 affects the stator current and, therefore, it is possible to monitor it in the current spectra. The radial
 98 motion generates harmonics in the stator current at frequencies given by (1)

$$99 \quad f_{\text{fault}} = |f_1 \pm n f_v| \quad (1)$$

100 where f_1 is the main supply frequency, n is an entire number and f_v is the vibration characteristic
 101 frequency. f_v depends on the type of bearing fault (outer or inner race, balls and train defect) with
 102 expressions that are function of the geometry and composition of the bearing [7].

103 The fault frequencies given by (1) are the result of taking into account the deviations in the main
 104 component of the airgap field. When the motor is fed by a power converter, the harmonics level is
 105 increased and so is the noise level, hampering the detection of the fault signatures. Nevertheless, the
 106 presence of these harmonics can be used to increase the available information also considering the
 107 deviations produced in the fields as a consequence of these harmonics. Even when the motor is
 108 directly fed from the line, since the supply is hardly ever perfectly sinusoidal, the number of fault
 109 signatures can be increased too considering the harmonic introduced by the supply. Therefore, (1)
 110 can be generalized by (2) where k is the order of the current harmonic.

$$111 \quad f_{\text{fault}} = |k f_1 \pm n f_v| \quad (2)$$

112 Considering (2), the number of fault signatures can be increased, resulting in a smaller or larger
 113 number of variables depending on the value of k and n . In [7,32] the first sideband around the 5th and
 114 7th harmonics is employed. In this paper, it is proposed to use a larger number of signatures,
 115 considering more harmonics, and other sidebands in addition to the first one as well. In the case study
 116 of Section 4, the first eleven current harmonics are used to feed the classifier, considering the first
 117 eleven sidebands around those harmonics. As each sideband is composed of two values, there are
 118 242 signatures for each characteristic bearing fault frequency, resulting in 968 signatures. Table 1
 119 summarizes the information regarding the proposed fault signatures and the comparison with the
 120 traditional approach.

121 **Table 1.** Bearing fault signatures considered in the traditional and in the proposed approach.

	Traditional approach	Proposed approach
Bearing fault frequencies	BPFO, BPFI, FTF; BSF	BPFO, BPFI, FTF; BSF
Harmonics considered	1	1, 2, ..., 11
Sidebands around harmonic	1	1, 2, ..., 11
Number of fault signatures	8	968

122

123 3. Diagnosis

124 The next step after selecting the candidate fault signatures is to choose and train the classifier.
 125 Many classification algorithms are available, with a wide variety of them already proposed to
 126 perform diagnosis tasks in induction motors. With the purpose of analyzing the improvement in the
 127 performance of the classifier when using the fault signatures presented in the previous section, the
 128 Matlab 2019a Classification learner App has been used. In this app there are available different types
 129 of classifiers: Decision trees, discriminant analysis, logistic regression classifiers, Naïve Bayes
 130 classifiers, support vector machines, nearest neighbor classifiers and ensemble classifiers. In each
 131 group, there are several classifiers available. Using these classifiers, it has been proved (as shown in
 132 the results section) the huge increase in performance of all the classifiers when using the 968 fault
 133 signatures instead of the usual 8 signatures.

134 However, when using such high number of signatures, and with a reduced number of tests, the
 135 risk of overfitting is certain. Shrinkage techniques allow to make use of all the predictors but
 136 shrinking the coefficients towards zero, hence, reducing variance [36]. If applied in linear models
 137 (which has the advantage in terms of interpretability of the model), it performs as follows: let x_i be
 138 the m predictors (or fault signatures in the context of condition monitoring) and y_i the response for

139 the n cases of the problem. A linear model tries to estimate the $m+1$ coefficients (b_0, \dots, b_m) . Using least
 140 squares fitting approach, b_i are selected to minimize (a).

$$141 \quad \sum_{i=1}^n (y_i - b_0 - \sum_{j=1}^m b_j x_{ij})^2 \quad (3)$$

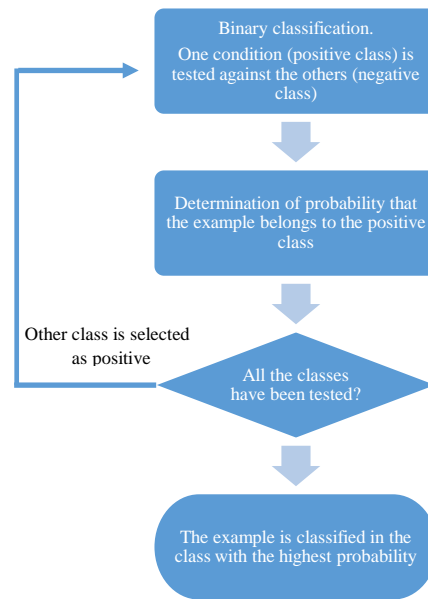
142 To perform the shrinkage, a second term is added to (a), $\lambda \sum_{j=1}^m b_j^2$, which acts as shrinkage
 143 penalty. Its influence depends on the value of λ , which is a tuning parameter that increases or
 144 decreases the penalty. For higher values of λ , the penalty grows and the coefficient estimated will
 145 tend to zero, which implies that the estimation is somehow penalized, sacrificing some of the
 146 performance on the training set but with the aim of improving its predictive capacity with future
 147 observations. The penalty applies to all the coefficients but the intercept, b_0 , since this term is just an
 148 estimation of the mean when the predictors are zero [36].

149 This way of applying the penalty so performing the shrinkage on the estimated coefficients is
 150 known as Ridge Regression. It has the disadvantage that the shrinkage is applied to all the coefficients
 151 but none of them are set to zero, so all the predictors are included in the solution, which for problems
 152 with a large number of predictors (as in the problem dealt in this paper) leads to lose the
 153 interpretability of the model. A way of tackling this problem is to change the penalty term into
 154 $\lambda \sum_{j=1}^m |b_j|$, or in statistical terms, to change an l_2 penalty for an l_1 one [36]. The use of an l_1 norm has
 155 the inconvenience of turning the function to minimize into non-differentiable, although there are
 156 available methods to proceed with the minimization, such as proximal gradient ones [37]. This way
 157 of considering the penalty gives rise to the method known as Lasso. As opposed to Ridge Regression,
 158 with Lasso, some variables are canceled, so performing as variable selection, depending the number
 159 of the variables to be selected on the value of λ (as λ grows, less variables are selected).

160 Lasso was first applied to linear regressions and lately is receiving much attention being
 161 proposed to regularize a wide variety of statistical models [38]. In accordance to Occam's razor
 162 principle, simpler models are preferable, as long as they predict well the training data, since they are
 163 more likely to generalize well to unseen data [39]. With this principle in mind, Logistic Regression
 164 has been chosen as base model in which to apply the shrinkage technique. Logistic regression is
 165 adapted to classification problems since has a discrete outcome. It is based on the logistic function
 166 given by (4) which is suitable to be used in classification since its outcome can be inferred as a
 167 probability since runs between 0 and 1, and its elongated S-shape offers the advantage that the same
 168 additional input influences less the outcome for values near zero or one [40,41]. For binary
 169 classification, a threshold value of 0.5 is defined to assign the outcome to one class or the other, which
 170 in condition monitoring would be healthy or faulty. When the aim is to distinguish among different
 171 states of failure there are several classes into which the outcome can be classified. This
 172 multiclassification is performed via the one-versus-all approach as represented in the flow chart in
 173 Figure 1. This way, several binary classifiers are trained (as many as classes), where each classifier
 174 confronts one class against the rest. Finally, the outcome is assigned to the class where the probability
 175 is highest.

$$176 \quad f(x) = (1 + e^{-x})^{-1} \quad (4)$$

177



178

179 **Figure 1.** Methodology for multiclass classification.180 **4. Results**181 *4.1 Test Bench*

182 The tested induction motor is a two pole pair squirrel cage motor, star connected, with a rated
 183 power of 0.75 kW at 400 V and a rated current of 1.9 A at a rated speed of 1395 RPM. The tests were
 184 performed at two levels load, low (almost no load) and high (rated speed) using a magnetic powder
 185 brake. The data were collect using a DAC PCI-6250 M model (16 analogue inputs - 16-bit 1 MS/s) of
 186 National Instruments and Hall effect sensors of LEM. The sampling frequency was 25 kHz with a
 187 sampling time of 10 s (steady state).

188 For different supply conditions were considered (Table 2). The first one (S1) represents the motor
 189 directly fed from a 400 V utility supply. Supply S2 is the motor fed by an inverter (ABB) at 50 Hz and
 190 with a switching frequency of 4 kHz. For S3, the operating frequency was changed to 25 Hz, and for
 191 S4 the switching frequency was established at 5 kHz).

192

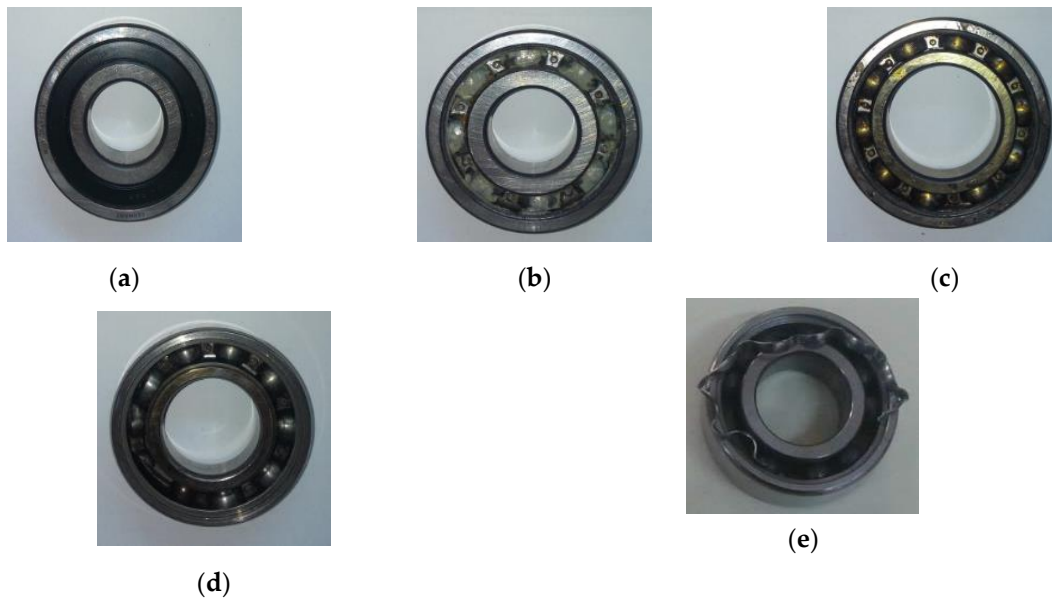
Table 2. Supplies tested.

Supply Identification	Power source	Operating frequency	Switching frequency
S1	utility	50 Hz	-
S2	Power converter	50 Hz	4 kHz
S3	Power converter	25 Hz	4 kHz
S4	Power converter	50 Hz	5 kHz

193

194 To initiate the tests, a new SKF Explorer 6004 bearing was used, performing the corresponding
 195 tests to represent the healthy condition. Then, to provoke the progressive wear of the bearing, the
 196 lubricant grease was contaminated using silicon carbide, a ceramic material with high resistance to
 197 erosion, corrosion and high thermal cycling. This process was established to simulate industrial
 198 environment conditions that lead to the degradation of the bearing such as inadequate lubrication,
 199 overloads or lubricant contamination (especially relevant to open bearings). During this process, five
 200 condition states were defined according to the degradation of the bearing, as summarized in Table 3.
 201 After assembling the new bearing, 20 tests per supply were run corresponding to the healthy state
 202 (C1). Then, the bearing was first contaminated and the motor run unloaded for 12 hours to lead the

203 bearing to the “incipient fault” condition (C2). In this condition, 15 tests were performed for each
 204 supply. The process of running the motor unloaded and contaminating the grease was repeated
 205 giving way to “intermediate fault” condition (C3), with 15 tests per supply, “developed fault” with
 206 10 tests (C4) and “complete breakdown” (C5) with 10 tests for each supply. Figure 2 presents pictures
 207 of the bearing in each of the conditions, showing the evolution of the fault along the tests.
 208



209 **Figure 2.** Evolution of the bearing along the tests: (a) healthy state, (b) incipient fault, (c) intermediate
 210 fault (d) developed fault (e) complete breakdown.

211

212

Table 3. Bearing conditions tested.

Condition	Evolution of the fault	Number of tests per supply
C1	healthy state	20
C2	incipient fault	15
C3	intermediate fault	15
C4	developed fault	10
C5	complete breakdown	10

213

214 4.2. Classification with 968 fault signatures

215 In order to show the improvement in the classification when using the whole of the fault
 216 signatures as proposed in Section 2, next the results obtained using the Matlab 2019a Classification
 217 learner App are presented. 5-fold cross validation was used. Table 4 summarizes the results obtained
 218 with the App with the accuracy for the classification in each of the five bearing conditions at low and
 219 high load. All the algorithms included in the App have been tested showing the one that has the best
 220 performance for each tested case (depending on the load and the supply) and its accuracy. The same
 221 procedure has been applied feeding the algorithms with eight inputs, following the traditional
 222 procedure of considering just the first sideband around the vibration characteristics frequencies,
 223 according to (2).
 224

225 **Table 4.** Comparison between the traditional (8 fault signatures) and proposed approach (968 fault
226 signatures) with the algorithms included in the Matlab 2019a Classification learner App.

Supply Identification	Load	Best accuracy	Best algorithm	Best accuracy	Best algorithm
		968 fault signatures	968 fault signatures	8 fault signatures	8 fault signatures
S1	Low	95.7 %	KNN ¹	40 %	SVM ²
	High	92.9 %	SVM ²	40 %	SVM ²
S2	Low	88.6 %	SVM ²	32.9 %	BT ⁵
	High	98.6 %	SVM ²	44.3 %	BT ⁵
S3	Low	81.4 %	BT ⁵	41.4 %	SVM ²
	High	97.1 %	LD ⁴	60 %	KNN ¹
S4	Low	85.7 %	LD ⁴	41.4 %	SVM ²
	High	98.6 %	BT ⁵	42.9 %	SVM ²

227 ¹ Fine KNN, ²Quadratic Support Vector Machines, ³Gaussian Naive Bayes, ⁴Linear Discriminant, ⁵Bagged Tress

228
229 According to the results shown in Table 4, it is very clear that the use of the fault signatures
230 related to a bigger number of sidebands around more harmonics outperforms the use of just eight
231 fault signatures. The huge improvement in the performance is observable in the all the cases, for the
232 different supplies, operating frequencies, switching frequencies and loads. The results are in general
233 better for high load since the energy associated to the harmonics is higher. It is also remarkable that
234 there is a variety of selected algorithms, being Support Vector Machines the most repeated although,
235 in some cases, Gaussian Naive Bayes, Linear Discriminant, Fine KNN and Bagged Trees perform
236 better. This discrepancy adds difficulty to the selection of a classifier valid for all the operating
237 conditions. An algorithm that performs well for all the cases would be desirable. Besides, as it was
238 stated earlier, the use of a big number of signatures (much bigger than the number of tests) may lead
239 to overfitting, losing the trained algorithms the ability to generalize when classifying new
240 observations. To take into account this situation, shrinkage is applied as explained in Section 3.

241 4.3. Classification with 968 fault signatures applying shrinkage

242 Previous section has shown that the classification improves hugely when more information
243 available in the spectra is considered. In this section, shrinkage methods are applied with the double
244 purpose of selecting an algorithm with good performance independently of the operating conditions
245 and of avoiding the problem of overfitting (prone to appear due to the high number of fault
246 signatures, much higher than the number of tests). As explained in Section 3, two different types of
247 shrinkage methods are considered: Ridge regression where all the inputs are considered in the
248 classification, and Lasso that performs variable selection (considering a higher or lower number of
249 inputs in the classification depending on the value of the penalty parameter). A third method is
250 included in the comparison, Elastic nets, which can be considered as a mixture between Lasso and
251 Ridge regression.

252 To build the algorithms and measure their performance, the data sets for each case study are
253 divided into two different sets, the training set consisting of 70% of the cases and the test set with the
254 other 30% of the data. Table 5 shows the performance, measured in terms of accuracy, for the three
255 shrinkage methods, for each supply and load. It can be observed that the results are very good for all
256 the cases, although with some differences in the performance among the cases analyzed, as it also
257 happened for the algorithms considered in the previous section. The three shrinkage methods
258 perform well, although in general, Lasso obtains the best accuracy, therefore, if a single method were
259 to be selected, Lasso would be the candidate. In this selection it has also been taken into account that,
260 since Lasso eliminates variables from the classifier, the model obtained gains in interpretability and
261 computational cost. For that reason, next, a deeper analysis on the performance of Lasso is presented,
262 taking especially into consideration the influence of the penalty parameter, since the number of
263 variables selected (and, consequently, the characteristics of the model) depend on this parameter.

264
265**Table 5.** Comparison of Accuracy (%) obtained using different methods of shrinkage with 968 fault signatures.

Supply Identification	Load	Lasso	Elastic Nets	Ridge Regression
S1	Low	100	100	100
	High	90.48	90.48	85.71
S2	Low	95.24	90.48	80.95
	High	95.24	100	100
S3	Low	80.95	76.19	76.19
	High	90.48	95.24	95.24
S4	Low	90.48	80.95	85.71
	High	100	95.24	85.71

266

267

268

269

270

271

272

273

274

275

276

277

278

279

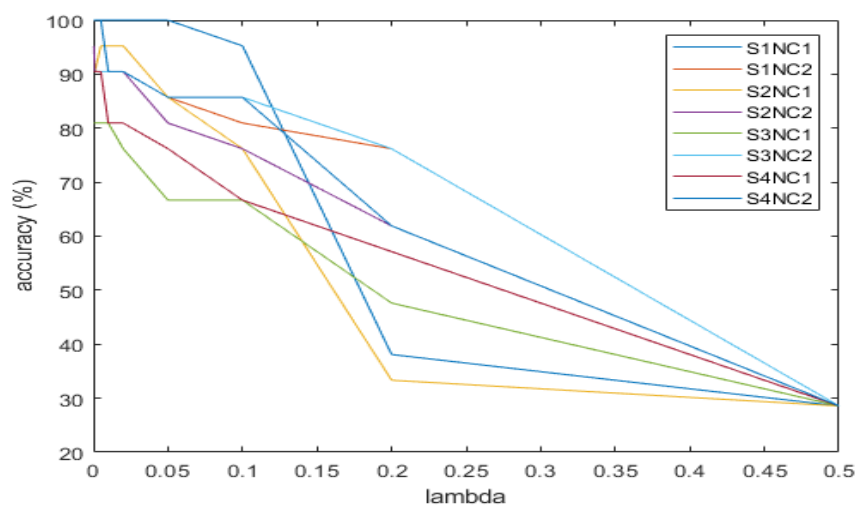
280

281

282

283

As it was stated in Section 3, the main way in which Lasso avoids overfitting is by feature selection, which is controlled by adjusting the regularization parameter λ . The bigger λ , more parameters b_j in (3) will be zero, that is, the corresponding predictors will not be considered when designing the classifier. Therefore, if a high value of λ is chosen, it is much less likely to result in overfitting, besides, the computational cost is highly reduced. The drawback is that, if less predictors are considered, the performance of the classifier will be reduced. Therefore, a trade-off must be reached to select the best value for the regularization parameter to obtain a good classifier performance with less computational cost. The selection of the value of the regularization parameter has been performed considering the train set. No additional validation set has been considered since the number of tests per case study is low and this would have led to training, validating and test sets with very few data in each one. Figure 3 shows the evolution of the accuracy depending on the regularization parameter and Table 6 shows the selected value for each supply and load condition. The value chosen for the classifier is the highest one that achieves the best accuracy for that supply and load, since for smaller values of λ the computational cost would be higher. If a unique value were to be chosen for all the supplies, 0.05 could be selected when operating at high load and 0.02 at low load. If the common value of 0.02 were to be chosen, the performance of the algorithm in this case would decrease around 5%, although the computational cost would decrease.



284

285

286

Figure 3. Performance of Lasso classifier depending on the value of the regularization parameter for different supplies (S1-S6) and loads (HL: high load, LL: low load).

287

288

289

Table 6. Regularization parameter selected for different supplies and level of load.

Supply	Load	Regularization parameter
S1	High	0.02
	Low	0.05
S2	High	0.0003
	Low	0.02
S3	High	0.01
	Low	0.01
S4	High	0.005
	Low	0.005

290

291

292

293

294

295

296

297

298

299

300

301

302

303

So far, accuracy has been used to measure the performance of the classifier. Obviously, from an algorithmic point of view, it is important to classify all the states correctly, and therefore to achieve the highest possible accuracy. However, from a condition monitoring point of view, some misclassifications are more relevant than others, being especially relevant to predict the first and fifth states correctly, that is, the healthy and completely faulty conditions. With this purpose, Tables 7-10 show the confusion matrices resulting from applying Lasso classifier for the four supplies and two load conditions. It can be observed how for the healthy state, for 48 instances (there are six true healthy states in each of the eight cases) only one case (S3, low load) is misclassified. And even if this case can be considered as a false negative, this instance is classified as an incipient fault, not as a more developed one. In the same way, for the 24 complete faulty cases (three for each of the eight cases) only one is misclassified (again, S3 at low load), being predicted as an intermediate fault. Finally, it is relevant to point out that for all the 168 cases to classify, 13 are not correctly classify but just four of them are classify more than one class away from the true class.

304

Table 7. Confusion matrices for supply S1 applying lasso classifier.

	True class	Low Load					High Load				
		Predicted class					Predicted class				
		C1	C2	C3	C4	C5	C1	C2	C3	C4	C5
C1	6	0	0	0	0	6	0	0	0	0	
C2	0	5	0	0	0	0	3	0	0	1	
C3	0	0	4	0	0	0	1	4	0	0	
C4	0	0	0	3	0	0	0	0	3	0	
C5	0	0	0	0	3	0	0	0	0	3	

305

306

Table 8. Confusion matrices for supply S2 applying lasso classifier.

	True class	Low Load					High Load				
		Predicted class					Predicted class				
		C1	C2	C3	C4	C5	C1	C2	C3	C4	C5
C1	6	0	0	0	0	6	0	0	0	0	
C2	1	3	0	0	0	0	3	0	0	1	
C3	0	0	5	0	0	0	1	4	0	0	
C4	0	0	0	3	0	0	0	0	3	0	
C5	0	0	0	0	3	0	0	0	0	3	

307

308

Table 9. Confusion matrices for supply S3 applying lasso classifier.

	True class	Low Load					High Load				
		Predicted class					Predicted class				
		C1	C2	C3	C4	C5	C1	C2	C3	C4	C5
C1	5	1	0	0	0	6	0	0	0	0	
C2	0	4	0	0	0	0	4	0	0	0	
C3	0	0	3	1	1	1	1	3	0	0	
C4	0	0	0	3	0	0	0	0	3	0	
C5	0	0	0	1	2	0	0	0	0	3	

309

310

Table 10. Confusion matrices for supply S4 applying lasso classifier.

	rue class	Low Load					High Load				
		Predicted class					Predicted class				
		C1	C2	C3	C4	C5	C1	C2	C3	C4	C5
C1	6	0	0	0	0	6	0	0	0	0	
C2	0	4	0	0	0	0	4	0	0	0	
C3	0	0	4	0	1	0	0	5	0	0	
C4	0	0	1	2	0	0	0	0	3	0	
C5	0	0	0	0	3	0	0	0	0	3	

311

312 5. Discussion

313 A procedure for the diagnosis of induction motor bearings has been presented. The main
 314 purpose of the proposal is to maintain the good performance of existing methods that use vibrations
 315 or sound as inputs but using the stator current. So far, the monitoring of the current has not achieved
 316 as good performance as the use of the other variables mentioned, but since has some clear advantages
 317 related to the necessary sensors it is advisable to have a procedure that allows to use the current. To
 318 achieve this goal it has been proposed to take advantage of more information that can be extracted
 319 from the spectra beyond what is commonly used, but with no extra computational cost.

320 It has been shown that the use of much more information greatly improved the performance of
 321 the diagnosis, which has been proved by means of 24 classifiers (available in the Matlab Classification
 322 learner app). However, it must be taken into account that detection and diagnosis are interlinked.
 323 There is no use in expecting a good diagnosis performance if the fault signatures obtained during the
 324 detection process are of a bad quality. Conversely, although there were high informative fault
 325 signatures, if the diagnosis stage is bad designed, the whole process will suffer. Besides, the chosen
 326 algorithm must be in accordance with the available variables. Therefore, it has been selected a type
 327 of classifier that can perform well with the particular conditions of the problem, where there are much
 328 more fault signatures that cases to classify. Shrinkage methods have been chose since they allow to
 329 perform in those condition avoiding the problem of overfitting.

330 Three shrinkage methods have been compared, Lasso, Ridge regression and Elastic nets and all
 331 of them have proved to achieve a very good performance in the cases analyzed. Although all three
 332 meet the expectations, Lasso has been chosen to analyze its results in greater depth since this method
 333 selects variables, providing simpler and more interpretable models. For the analysis of the
 334 performance of Lasso, the confusion matrices for eight different scenarios have been provided and
 335 analyzed. Although from an algorithmic point of view, it is important to classify all the states
 336 correctly, from a maintenance perspective, it is especially relevant the presence of false positives or
 337 false negatives concerning the healthy and complete fault conditions. That is, some misclassifications

338 are more relevant than others are. For example, wrong predictions between conditions corresponding
339 to intermediate and incipient faults are not likely to have important repercussions but, on the
340 contrary, a misclassification between states healthy and complete fault will surely have further
341 implications. It has been shown that the predictions obtained with the proposed method matches the
342 expectations from a condition monitoring perspective.

343 **Author Contributions:** Conceptualization, Oscar Duque-Perez, Daniel Morinigo-Sotelo and Wagner Fontes
344 Godoy; Data curation, Wagner Fontes Godoy; Methodology, Oscar Duque-Perez; Software, Carlos Del Pozo-
345 Gallego; Validation, Daniel Morinigo-Sotelo; Writing – original draft, Oscar Duque-Perez; Writing – review &
346 editing, Daniel Morinigo-Sotelo.

347 References

- 348 1. Immovilli, F.; Bellini, A.; Rubini, R.; Tassoni, C. Diagnosis of bearing faults in induction machines by
349 vibration or current signals: A critical comparison. *IEEE Trans. Ind. Appl.* **2010**, *46-4*, 1350–1359.
- 350 2. Henao H. et al. Trends in fault diagnosis for electrical machines. *IEEE Ind. Electron. Mag.*, **2014**, *8-2*, 31–42.
- 351 3. Akin, B.; Toliyat, H.A.; Orguner, U.; Rayner, M. PWM Inverter Harmonics Contributions to the Inverter-
352 Fed Induction Machine Bearing Fault Diagnosis. in IEEE Applied Power Electronics Conference, APEC
353 2007 - Twenty Second Annual, pp. 1393-399.
- 354 4. Bellini, A.; Filippetti, F.; Tassoni, C.; Capolino, G.-A.. Advances in diagnostic techniques for induction
355 machines. *IEEE Trans. Ind. Electron.*, **2008**, *55-12*, 4109–4126.
- 356 5. Zarei, J.; Poshtan, J. An advanced Park's vectors approach for bearing fault detection. *Tribology International*
357 **2009** *42*, 213–219.
- 358 6. Blodt, M.; Granjon, P.; Raison, B.; Rostaing, G. Models for bearing damage detection in induction motors
359 using stator current monitoring. *IEEE Trans. Ind. Electron.*, **2008**, *55-4*, 1813–1822.
- 360 7. Duque, O.; Pérez, M.; Morínigo, D. Detection of bearing faults in cage induction motors fed by frequency
361 converter using spectral analysis of line current in IEEE International Conference on Electric Machines and
362 Drives, 2005 pp. 17-22.
- 363 8. Zhou, W.; Habetler, T.G.; Harley, R.G. Bearing Fault Detection Via Stator Current Noise Cancellation and
364 Statistical Control. *IEEE Trans. Ind. Electron.*, **2008**, *55-12*, 4260–4269.
- 365 9. Singh, S.; Kumar, A.; Kumar N. Motor Current Signature Analysis for Bearing Fault Detection in
366 Mechanical Systems. *Procedia Materials Science*, **2014**, *6*, pp.171–177.
- 367 10. Deekshit Kompella, K.C.; Venu Gopala Rao, M.; Srinivasa Rao, R. DWT based bearing fault detection in
368 induction motor using noise cancellation. *Journal of Electrical Systems and Information Technology*, **2016**, *3-3*,
369 411–427.
- 370 11. Rosero, J.; Cusido, J.; Garcia Espinosa, A.; Ortega J. A.; Romeral, L. Broken Bearings Fault Detection for a
371 Permanent Magnet Synchronous Motor under non-constant working conditions by means of a Joint Time
372 Frequency Analysis in IEEE International Symposium on Industrial Electronics, 2007. ISIE 2007, pp. 3415-
373 3419.
- 374 12. Kablaa, A.; Mokrani, K. Bearing fault diagnosis using Hilbert-Huang transform (HHT) and support vector
375 machine (SVM). *Mechanics & Industry*, **2016**, *17-3*.
- 376 13. Camarena-Martinez, D.; Osornio-Rios, R.; Romero-Troncoso, R.J.; Garcia-Perez, A. Fused Empirical Mode
377 Decomposition and MUSIC Algorithms for Detecting Multiple Combined Faults in Induction Motors.
378 *Journal of Applied Research and Technology*, **2015**, *13-1*, 160-167.
- 379 14. Boudinar, A.H.; Benouzza, N.; Bendiabdellah, A.; Khodja, A. Induction Motor Bearing Fault Analysis
380 Using a Root-MUSIC Method. *IEEE Trans. Ind. Appl.*, **2016**, *52-5*, 3851–3860.
- 381 15. Arkan, M.; Çaliş, H.; Tağluk, M.E. Bearing and misalignment fault detection in induction motors by using
382 the space vector angular fluctuation signal. *Electrical Engineering*, **2005**, *87-4*, 197–206.
- 383 16. Godoy, W.F.; da Silva, I.N.; Goedtel, A.; Palácios, R.H.C.; Gongora, W.S. Neural approach for bearing fault
384 classification in induction motors by using motor current and voltage, in IEEE International Joint
385 Conference on Neural Networks (IJCNN), 2014, pp. 2087 – 2092.
- 386 17. Ballal, M.S.; Khan, Z.J.; Suryawanshi, H.M.; Sonolikar, R.L. Adaptive Neural Fuzzy Inference System for
387 the Detection of Inter-Turn Insulation and Bearing Wear Faults in Induction Motor. *IEEE Trans. Ind.*
388 *Electron.*, **2007**, *54-1*, 250–258.

- 389 18. Zarei, J.; Arefi, M.M.; Hassani, H. Bearing fault detection based on interval type-2 fuzzy logic systems for
390 support vector machines in 6th International Conference on Modeling, Simulation and Applied
391 Optimization (ICMSAO), 2015, pp. 1 – 6.
- 392 19. Salem, S.B.; Bacha, K.; Chaari, A. Support vector machine based decision for mechanical fault condition
393 monitoring in induction motor using an advanced Hilbert-Park transform. *ISA Transactions*, **2012**, 51-5, 566-
394 572.
- 395 20. Bouguerne, A. ; Lebaroud, A.; Medoued A.; Boukadoum, A. Classification of induction machine faults by
396 K-nearest neighbor in 7th International Conference on Electrical and Electronics Engineering (ELECO),
397 2011, pp. I-363-I-366
- 398 21. Tian, J.; Morillo, C.; Azarian M.H.; Pecht, M. Motor Bearing Fault Detection Using Spectral Kurtosis-Based
399 Feature Extraction Coupled With K-Nearest Neighbor Distance Analysis. *IEEE Trans. Ind. Electron.*, **2016**,
400 63-3, 1793–1803.
- 401 22. Farajzadeh-Zanjani, M.; Razavi-Far, R.; Saif, M. Diagnosis of Bearing Defects in Induction Motors by Fuzzy-
402 Neighborhood Density-Based Clustering in IEEE 14th International Conference on Machine Learning and
403 Applications, 2015, pp. 935-940.
- 404 23. Peng H.-W.; Chiang, P.-J. Control of mechatronics systems: Ball bearing fault diagnosis using machine
405 learning techniques in 8th Asian Control Conference (ASCC), 2011, pp. 175-180.
- 406 24. Santos, S.P.; Costa, J.A.F. A Comparison between Hybrid and Non-hybrid Classifiers in Diagnosis of
407 Induction Motor Faults in 11th IEEE International Conference on Computational Science and Engineering,
408 CSE '08, 2008, pp. 301-306.
- 409 25. Ergin, S.; Tezel, S.; Gulmezoglu, M.B. DWT-based fault diagnosis in induction motors by using CVA in
410 International Symposium on Innovations in Intelligent Systems and Applications (INISTA), 2011, pp. 129–
411 132.
- 412 26. Cunha Palácios, R.H.; da Silva, I.N.; Goedtel, A.; Godoy, W.F. A comprehensive evaluation of intelligent
413 classifiers for fault identification in three-phase induction motors. *Electric Power Systems Research*, **2015**, 127,
414 249–258.
- 415 27. Sugumaran, V.; Ramachandran, K.I. Automatic rule learning using decision tree for fuzzy classifier in fault
416 diagnosis of roller bearing. *Mechanical Systems and Signal Processing*, **2007**, 21-5, 2237-2247.
- 417 28. Zeng, M.; Yang, Y.; Zheng, J.; Cheng, J. Maximum margin classification based on flexible convex hulls for
418 fault diagnosis of roller bearings. *Mechanical Systems and Signal Processing*, **2016**, 66-67, 533–545.
- 419 29. Mbo’o, C.P.; Hameyer, K. Fault Diagnosis of Bearing Damage by Means of the Linear Discriminant
420 Analysis of Stator Current Features From the Frequency Selection. *IEEE Trans. Ind. App.*, **2016**, 52-5, 3861-
421 3868.
- 422 30. Montechiesi, L.; Cocconcelli, M.; Rubini, R. Artificial immune system via Euclidean Distance Minimization
423 for anomaly detection in bearings. *Mechanical Systems and Signal Processing*, **2016**, 76, 380-393.
- 424 31. Wang, D. An extension of the infograms to novel Bayesian inference for bearing fault feature identification.
425 *Mechanical Systems and Signal Processing*, **2016**, 80, 19–30.
- 426 32. Frosini, L.; Bassi, E.; Fazzi, A.; Gazzaniga, C. Use of the stator current for condition monitoring of bearings
427 in induction motors in Proceedings of the 2008 International Conference on Electrical Machines, 2008, pp.
428 1-6.
- 429 33. Morinigo-Sotelo, D.; Duque-Perez, O; Perez-Alonso, M. Assessment of the lubrication condition of a
430 bearing using spectral analysis of the stator current in International Symposium on Power Electronics
431 Electrical Drives Automation and Motion (SPEEDAM), 2010, pp. 1160 - 1165.
- 432 34. Domingos, P. *The Master Algorithm*. Basic Books, New York, 2015.
- 433 35. Benbouzid, M. E. H.; Kliman, G. B. What stator current processing based technique to use for induction
434 motor rotor faults diagnosis? *IEEE Trans. Energy Convers.*, **2003**, 18-2, 238–244.
- 435 36. James, G.; Witten, D.; Tibshirani, T.H.R. *An introduction to statistical learning* Springer 2013.
- 436 37. Amaral Santos, P.L.; Imangaliyev, S.; Schutte, K.; Levin, E. Feature selection via co-regularized sparse-
437 group Lasso. in *Machine learning, optimization and big data*, P.M Pardalos, P. Conca, G. Giuffrida and G.
438 Nicosi, Eds. Springer, 2016, pp. 118-131.
- 439 38. Tibshirani, D R. Regression shrinkage and selection via the lasso: a retrospective. *J. R. Statist. Soc. B*, **2011**,
440 73-3,273–282.
- 441 39. Zhang, X. Regularization. In *Encyclopedia of Machine Learning*. 2010 Edition. | Editors: Claude Sammut,
442 Geoffrey I. Webb. Springer, Boston, MA, 2010

- 443 40. Kleinbaum, G.; Klein, M. *Logistic Regression*. 3rd ed.; Springer Science+Business Media New York, 2010.
- 444 41. Pampel, F.C. *Logistic Regression. A Primer*. Sage Publications. 2000.